Acta Cryst. (1994). D**50**, 596–602

Crystallization and X-ray Structure Determination of Cytochrome c_2 from *Rhodobacter sphaeroides* in Three Crystal Forms

BY HERBERT L. AXELROD AND GEORGE FEHER*

Department of Physics, 0319, *University of California, San Diego, La Jolla, California* 92093-0319, *USA*

JAMES P. ALLEN

Department of Chemistry and Biochemistry, Arizona State University, Tempe, Arizona 85287-1604, *USA*

AND ARTHUR J. CHIRINO, MICHAEL W. DAY, BARBARA T. HSU AND DOUGLAS C. REES

Division of Chemistry and Chemical Engineering 147-75*CH*, *California Institute of Technology, Pasadena, California* 91125, *USA*

(*Received* 15 *November* 1993; *accepted* 31 *January* 1994)

Abstract

Cytochrome c_2 serves as the secondary electron donor that reduces the photo-oxidized bacteriochlorophyll dimer in photosynthetic bacteria. Cytochrome c_2 from *Rhodobacter sphaeroides* has been crystallized in three different forms. At high ionic strength, crystals of a hexagonal space group ($P6_122$) were obtained, while at low ionic strength, triclinic ($P1$) and tetragonal ($P4_12_12$) crystals were formed. The three-dimensional structures of the cytochrome in all three crystal forms have been determined by X-ray diffraction at resolutions of 2.20 Å (hexagonal), 1.95 Å (triclinic) and 1.53 Å (tetragonal). The most significant difference observed was the binding of an imidazole molecule to the iron atom of the heme group in the hexagonal structure. This binding displaces the sulfur atom of Met100, which forms the axial ligand in the triclinic and tetragonal structures.

Introduction

Cytochromes form a ubiquitous class of proteins that serve as electron carriers in different energy-transducing systems (reviewed in Moore & Pettigrew, 1990). In the purple non-sulfur photosynthetic bacterium *Rb. sphaeroides*, cytochrome c_2 is a 14 kDa water-soluble protein that contains one covalently bound heme as its prosthetic group (Vernon & Kamen, 1954). This cytochrome, along with the membrane-bound photosynthetic reaction center (RC) and cytochrome bc_1, carry out the photosynthetic electron-transfer processes in *Rb. sphaeroides* (reviewed by Nicholls & Ferguson, 1992). The cytochrome c_2 serves as the secondary electron donor that upon binding to the periplasmic surface of the RC transfers an electron to the photo-oxidized bacteriochlorophyll dimer (D^+) (Prince, Cogdell & Crofts, 1974; Prince, Baccarini-Melandri, Hauska, Melandri & Crofts, 1975; Overfield, Wraight & Devault, 1979; Rosen, Okamura & Feher, 1980; Rosen, Okamura, Abresch, Valkris & Feher, 1983). The oxidized ferricytochrome c_2 is re-reduced by cytochrome bc_1 to regenerate ferrocytochrome c_2 (reviewed in Crofts & Wraight, 1983).

The X-ray crystal structures of the RC from two photosynthetic bacteria, *Rhodopseudomonas viridis* (Deisenhofer, Epp, Miki, Huber & Michel, 1985) and *Rb. sphaeroides* (Allen *et al.*, 1986; Chang *et al.*, 1986; Allen, Feher, Yeates, Komiya & Rees, 1987; Chang, El-Kabbani, Tiede, Norris & Schiffer, 1991) have been determined. In *Rps. viridis*, a tetraheme cytochrome is permanently bound to the RC (Thornber, Olson, Williams & Clayton, 1969; Deisenhofer, Epp, Miki, Huber & Michel, 1985). In *Rb. sphaeroides*, cytochrome c_2 is an exogenous water-soluble protein that forms a transient complex with the RC. To understand the structure of the complex and the mechanism of electron transfer, a knowledge of the cytochrome structure is essential.

Different docking models for the interaction between cytochrome c_2 from *Rb. sphaeroides* and the RC have been proposed (Allen, Feher, Yeates, Komiya & Rees, 1987; Tiede & Chang, 1988; Caffrey, Bartsch & Cusanovich, 1992). In all the models negatively charged glutamic and aspartic acid side chains on the periplasmic surface of the RC were postulated to interact with positively charged side chains on the cytochrome. Since the X-ray structure of the cytochrome c_2 from *Rb. sphaeroides* was not available, these docking models relied on the known structures of homologous cytochromes from two other species of purple photosynthetic bacteria,

* To whom correspondence should be addressed.

Rhodospirillum rubrum (Salemme, Freer, Xuong, Alden & Kraut, 1973) and *Rhodobacter capsulatus* (Benning *et al.*, 1991). In this work, we describe the structure determination of cytochrome c_2 from *Rb. sphaeroides* in three different crystal forms prepared under different crystallization conditions. Preliminary accounts of this work have been presented (Allen, 1988; Axelrod *et al.*, 1992*a*,*b*).

Experimental procedures

Purification of cytochrome c_2

Cytochrome c_2 from *R. sphaeroides* was obtained from an overproducing strain cycA1, harboring the plasmid pC2P404.1 (Brandner, McEwan, Kaplan & Donohue, 1989). Cell growth and harvest were performed as described by Feher & Okamura (1978); periplasmic extracts containing cytochrome c_2 were prepared according to Rott, Fitch, Meyer & Donohue (1992). The cytochrome was purified as described by Bartsch (1978) with the following modifications: The cytochrome c_2 was precipitated from the periplasmic extract by 100% saturated $(NH_4)_2SO_4$. The resulting pellet was applied to a hydrophobic column (*n*-butyl-Toyopearl 250S from Toso-Haas) equilibrated with 60% saturated $(NH_4)_2SO_4$. Following a wash with the equilibration salt (five volumes), the cytochrome was eluted from the column with 40% saturated $(NH_4)_2SO_4$ and dialyzed against 10 m*M* TE buffer.* Two additional chromatographic steps with an anion exchange column [dimethylaminoethyl (DEAE)-Toyopearl 250S] and a cation exchange column [carboxymethyl (CM)-Toyopearl 250S] were then carried out. The purified cytochrome was dialyzed against a solution containing the crystallization buffer (see below). The protein was concentrated as needed by centrifuging in Centricon 10 (Amicon) tubes. The concentration of cytochrome was determined spectroscopically using an extinction coefficient $\varepsilon_{550} = 30.8\ mM^{-1}\ cm^{-1}$ for the reduced form of the protein (Bartsch, 1978). The purity of the cytochrome was determined from the ratio of its absorbance at 280 nm to that at 417 nm (Bartsch, 1978). Solutions with ratios less than 0.25 were used for crystallization. The absence of protein contaminants was verified by sodium dodecyl sulfate polyacrylamide gel electrophoresis (SDS–PAGE) in 15% polyacrylamide gels.

* TE buffer = 10 m*M* TRIS [tris(hydroxymethyl)aminomethane], 1 m*M* EDTA (ethylenediaminetetraacetic acid), pH 8.0.

Crystallization

The crystallization of cytochrome c_2 was accomplished by the hanging-drop technique (McPherson, 1982). The crystallization protocols for the three different crystal forms were as follows.

(1) *Hexagonal crystallization.* 10 μl droplets containing cytochrome c_2 at a concentration of 10 mg ml^{-1}, 100 m*M* imidazole (pH 7.0) and 30% saturated $(NH_4)_2SO_4$ were equilibrated against 1 ml reservoirs containing 70% saturated $(NH_4)_2SO_4$ in 100 m*M* imidazole (pH 7.0). Crystals were observed within one week at a thermostatically controlled temperature of 4 °C; they reached a length of 1.5 mm within three weeks. This crystal form has been previously reported by Allen (1988).

(2) *Triclinic crystallization.* 10 μl droplets containing 10 mg ml^{-1} cytochrome c_2, 10 m*M* HEPES (*N*-2-hydroxyethyl-piperazine-*N*′-2-ethanesulfonic acid) (pH 7.0) and 5%(*w*/*v*) PEG (polyethylene glycol) 4000 (EM Science) were equilibrated against 1 ml reservoirs containing an unbuffered solution of 20%(*w*/*v*) PEG 4000. Crystals were observed at ambient (22 °C) temperature after three weeks.

(3) *Tetragonal crystallization.* 10 μl droplets containing 15 mg ml^{-1} cytochrome c_2, 50 m*M* MES [2-(*N*-morpholino)ethanesulfonic acid] (pH 6.0) and 5%(*w*/*v*) PEG 4000 were equilibrated against 1 ml reservoirs containing 50 m*M* MES (pH 6.0), 20%(*w*/*v*) PEG 4000 and 0.6 *M* NaCl. Crystals were

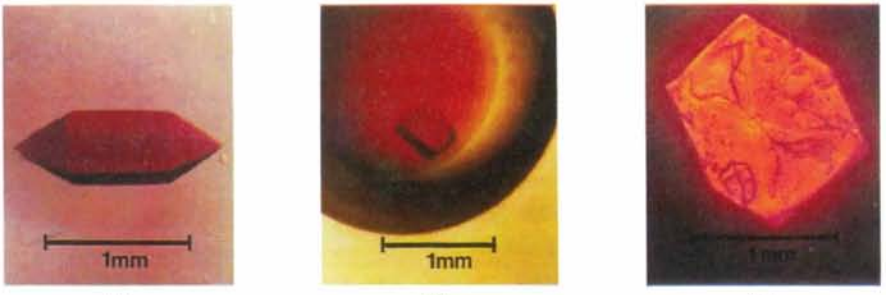

Fig. 1. Three different crystal forms of cytochrome c_2 from *Rhodobacter sphaeroides*. (*a*) Hexagonal crystal (space group $P6_122$) that grew at 4 °C from an imidazole-buffered solution of $(NH_4)_2SO_4$; (*b*) triclinic crystal (space group $P1$) that grew at 22 °C from a low ionic strength (10 m*M*) solution of PEG 4000; (*c*) tetragonal crystal (space group $P4_12_12$) that grew at 22 °C in 50 m*M* MES buffer. Photographed with polarized light.

formed within one week at ambient (22 °C) temperature.

Phasing and refinement

X-ray diffraction data were collected from all three crystal forms. The primary phasing necessary for the calculation of initial electron-density maps was first accomplished for the hexagonal crystal form. The derivatized form used for the phase determination was obtained by soaking the crystals for 14 d at 22 °C in a 90% saturated $(NH_4)_2SO_4$, 100 m*M* imidazole (pH 7.0), 40 m*M* trimethyllead acetate (Holden & Rayment, 1991) solution.

(1) *Hexagonal crystal form.* From X-ray diffraction data of the native and trimethyllead acetate derivative, isomorphous-difference Patterson and anomalous-difference Patterson maps were calculated with the program *ROCKS* (Reeke, 1984). From these, the lead sites were located, the phasing information was obtained, and an electron-density map was calculated.

From the electron density, a tracing of the overall fold of the polypeptide backbone as well as the placement of the heme porphyrin ring was obtained. Model building, using the known amino-acid sequence of *Rb. sphaeroides* cytochrome c_2 (Ambler *et al.*, 1979) was performed on an Evans and Sutherland PS330 computer graphics terminal with the interactive molecular modeling program *FRODO* (Jones, 1985). Least-squares refinement of the starting model was performed with the program *TNT* (Tronrud, TenEyck & Matthews, 1987). Further rounds of coordinate and *B*-factor refinements were performed after rebuilding the model against $2F_{obs} - F_{calc}$ and $F_{obs} - F_{calc}$ electron-density maps. Simulated-annealing refinement with the program *X-PLOR* (Brünger, Kuriyan & Karplus, 1987) was used as the last refinement step. The *R* factor* for the current model, including 52 water molecules, is 17.0% using all observed X-ray diffraction data within the resolution range 6.0–2.2 Å (r.m.s. deviations from ideal bond lengths = 0.010 Å and bond angles = 1.9°).

(2) *Triclinic crystal form.* The coordinates of the cytochrome c_2 in the hexagonal space group were used as a molecular-replacement model to determine the structure of the cytochrome at higher resolution in the triclinic space group. Molecular-replacement calculations were carried out with the integrated software package *MERLOT* (Fitzgerald, 1988) and a translation function program *GENTF* (D. Rees, unpublished). These calculations established that both cytochrome c_2 molecules within the triclinic unit cell were situated in similar orientations, and that the triclinic crystal form of the cytochrome c_2 from *Rb. sphaeroides* is pseudo-body centered. The molecular replacement solution was refined by rigid-body refinement using *TNT*, followed by refinement with *X-PLOR* leading to an *R* factor, including 204 water molecules, of 17.3% (r.m.s. bond-length deviation = 0.010 Å and r.m.s. bond-angle deviation = 1.9°).

(3) *Tetragonal crystal form.* The coordinates of the cytochrome in the triclinic space group, refined to a resolution of 1.95 Å, were used to determine the structure of the cytochrome in the tetragonal space group at a resolution of 1.6 Å. Rotation and translation functions were calculated within the resolution range 8–3 Å with the *MERLOT* program. The translation function indicated that these crystals of the cytochrome belong to space group $P4_12_12$. Refinement of the tetragonal model at a resolution of 1.6 Å was performed with the program *TNT* and *X-PLOR*, as described for the hexagonal and triclinic forms. The current *R* factor, including 25 water molecules is 22.5% (r.m.s. bond-length deviation = 0.010 Å and r.m.s. bond-angle deviation = 1.8°).

Table 1. *Crystal forms of cytochrome c_2 from Rb. sphaeroides*

Crystal form	Space group	Unit-cell parameters (Å, °)	Molecules per asymmetric unit	V_m (Å^3 Da^{-1})
Hexagonal	$P6_122$	$a = b = 64.3$ $c = 163.4$ $\alpha = \beta = 90$ $\gamma = 120$	1	3.5
Triclinic	$P1$	$a = 45.3$ $b = 38.1$ $c = 37.5$ $\alpha = 102.3$ $\beta = 72.4$ $\gamma = 90.6$	2	2.1
Tetragonal	$P4_12_12$	$a = b = 82.3$ $c = 37.6$ $\alpha = \beta = \gamma = 90$	1	2.3

Results and discussion

The three different crystal forms of cytochrome c_2 from *Rb. sphaeroides* are shown in Fig. 1. At high ionic strength, crystals belonging to the hexagonal crystal system (Fig. 1*a*) were obtained, while at low ionic strength, both triclinic (Fig. 1*b*) as well as tetragonal crystals (Fig. 1*c*) formed. The crystal parameters are summarized in Table 1. The Matthews number, V_m (Matthews, 1968) of the hexagonal form is the largest, implying that this form has the highest solvent content. This high solvent content may account for the diminished resolution of the hexagonal form (2.2 Å) as compared to the triclinic (2.0 Å) and tetragonal (1.5 Å) forms (see Table 2).

The packing motif in the crystal forms is different. In the triclinic form, which is pseudo-body centered, subunit interactions exist between pseudo-translational symmetry-related cytochromes in identical

* $R = (\sum_{hkl} F_{obs} - F_{calc}|)/\sum_{hkl} F_{obs}$, where F_{obs} represents the observed scattering-factor amplitude and F_{calc} is the scattering-factor amplitude calculated from model coordinates.

Table 2. *Summary of X-ray diffraction data for cytochrome c_2 from Rb. sphaeroides*

Crystal form	Detector type	Resolution (Å)	Unique reflections	% Completeness	R_{symm}*
Native hexagonal†	Siemens X-1000‡	2.70	5375	88.4	0.054
Native hexagonal†	Rigaku R-AXIS II§	2.20	10348	84.8	0.046
Trimethyllead acetate derivative hexagonal†	Siemens X-1000‡	2.70	5387	89.0	0.062
Native triclinic†	Siemens X-1000‡	1.95	14690	77.2	0.056
Native tetragonal†	Siemens X-1000‡	1.53	18286	91.7	0.073

* $R_{symm} = (\sum_{hkl}\sum_N \langle I_{hkl}\rangle - I_{hkl})/\sum_{hkl}\sum_N I_{hkl}$, where I_{hkl} is the reflection intensity and $\langle I_{hkl}\rangle$ is the mean intensity for the set of N symmetry-equivalent reflections.

† Data were collected from a single crystal.

‡ Data were processed with the *XENGEN* program (Howard *et al.*, 1987).

§ Data were processed with the program *PROCESS* (Higashi, 1990).

orientations. Most of these lattice contacts in the triclinic form are hydrogen bonds between residues located on surface loops of the protein. In contrast, in the tetragonal form, contacts between subunits in identical orientations do not exist, and most of the contacts are between the N-terminal region of one cytochrome and the C-terminal region of a symmetry-related subunit. Packing differences between the triclinic and tetragonal forms may be influenced by pH. Crystallization of the cytochrome in the tetragonal form at pH 6.0 occurs at a value closer to the reported pI of 5.5 (Meyer, 1970). In the tetragonal form, the side chain of Glu2 (near the N terminus) on the cytochrome makes electrostatic contact with the side chain of His111 (near the C terminus) on a symmetry-related molecule. In the triclinic form, crystallized at pH 7.0, His111 with an expected pK_a of ~6.0 is less likely to form packing interactions. In the hexagonal crystal, the binding of imidazole (from the crystallization buffer) is believed to influence packing (see later discussion). For example, the displaced side chain of Met100 is within van der Waals contact of Phe102 on a symmetry-related subunit.

X-ray diffraction data were collected from native crystals of the three forms, and from the trimethyllead acetate derivative of the hexagonal form (Table 2). The resulting difference Patterson map calculated for the hexagonal crystal derivative indicated one major trimethyllead acetate binding site. The coordinates of the identified major lead binding site were refined utilizing the program *HEAVY* (Terwilliger & Eisenberg, 1983). Two additional minor sites were located in difference Fourier maps. Further refinement of coordinate, occupancy and isotropic temperature factor for the three lead sites, resulted in single isomorphous replacement anomalous-scattering (SIRAS) phases at 3.0 Å resolution with an overall figure of merit* of 0.77 and a phasing power† of 3.33. Based on these lead derivative phases, electron-density maps at a resolution of 3 Å were calculated in both the $P6_122$ and the $P6_522$ space groups. The boundaries of the protein subunits and the prosthetic heme group could be observed only in the electron-density maps calculated in the $P6_122$ enantiomorph. These maps were used for the initial model building which was then subjected to several refinement cycles, leading to an R factor of 17.0%.

The model of the *Rb. sphaeroides* cytochrome c_2 in the hexagonal space group is shown in Fig. 2. The model has the following secondary-structure elements; five α-helices, eight surface loops, an anti-parallel β-loop, and a short stretch of anti-parallel β-sheet (Fig. 2); at the N terminus, amino-acid residues 5–17 form a distorted α-helix. Another stretch of α-helix exists toward the C-terminal end of the cytochrome between Glu107 and Gln119. These N- and C-terminal α-helices are spatially in close

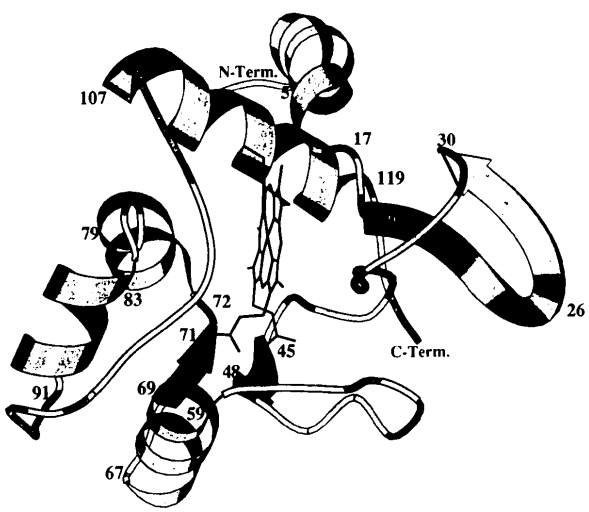

Fig. 2. The structure of cytochrome c_2 from *Rb. sphaeroides*. A ribbon representation of the polypeptide folding and prosthetic heme group of cytochrome c_2 from *Rb. sphaeroides* based on the refined hexagonal crystal structure. The model was generated with the graphics program *MOLSCRIPT* (Kraulis, 1991). In the orientation shown, the solvent-exposed edge of the porphyrin ring faces the viewer.

* The figure of merit is the mean value of the cosine of the error in the phase angle.

† Phasing power = f_h/E where f_h is the root-mean-square heavy-atom structure-factor amplitude and E is the root-mean-square lack-of-closure error.

proximity, as was also found for other *c*-type cytochromes (Moore & Pettigrew, 1990, ch. 4). The hydrophobic side chains of two conserved residues, Phe12 on the N-terminal α-helix and Tyr116 on the C-terminal α-helix, are within van der Waals contact. Three additional α-helical segments exist between amino-acid residues 59–67, 72–79 and 83–91. The β-loop of cytochrome c_2 lies between residues 20–30. This antiparallel β-loop is stabilized by four hydrogen bonds, and at the tip of this β-loop, between Asp23 and Gly26, a type I (Venkatachalan, 1968) reverse turn exists. In addition to this anti-parallel β-loop, interstrand hydrogen bonding between Gly45–Ala48 and Leu69–Trp71 forms a short antiparallel β-sheet.

The main structural differences between cytochrome c_2 from *Rb. sphaeroides* and cytochrome c_2 from *R. rubrum* (Salemme, Freer, Xuong, Alden &

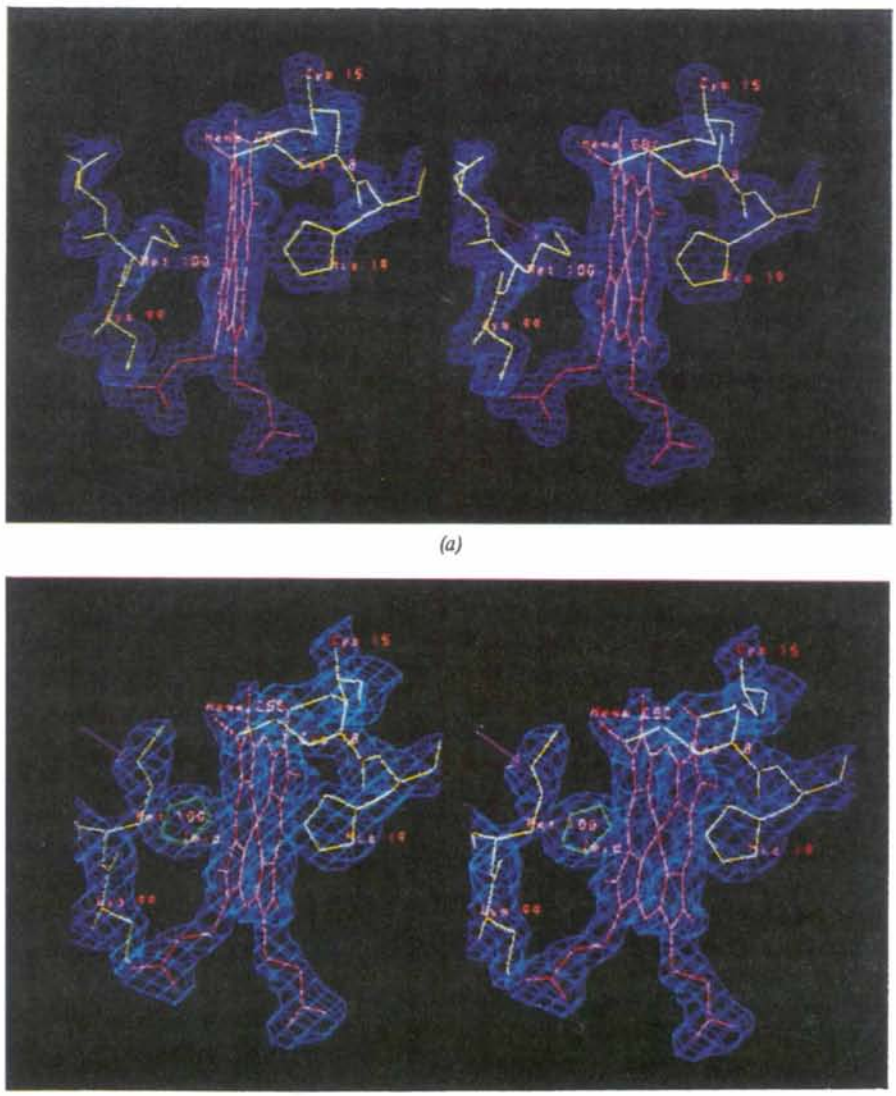

Fig. 3. Stereoview of $2F_{obs} - F_{calc}$ electron density surrounding the prosthetic heme group and the axial ligands in the triclinic (*a*) and hexagonal (*b*) crystal forms of cytochrome c_2. F_{obs} designates the structure-factor amplitudes from the observed X-ray diffraction data and F_{calc} the structure-factor amplitudes calculated from the refined coordinates. (*a*) $2F_{obs} - F_{calc}$ electron density for the triclinic crystal form calculated at a resolution of 2 Å and contoured at 2σ above the mean level of the map. The S atom of Met100 (arrow) is 2.3 Å from the heme Fe atom in the triclinic and tetragonal (not shown) crystal structures. Coordination to the heme is indicated by the continuous electron density from the side chain of Met100 to the heme Fe atom. (*b*) $2F_{obs} - F_{calc}$ electron density calculated at a resolution of 2.2 Å and contoured at 2σ above the mean level of the map for the hexagonal crystal form of the cytochrome. Electron density associated with the side chain of Met100 is discontinuous with the porphyrin density, with the S atom of Met100 (arrow) 5.7 Å displaced from the heme Fe atom. An imidazole (originating from the buffer) is bound to the iron. Its position (labeled Imid) is shown together with its associated electron density.

Kraut, 1973) and *Rb. capsulatus* (Benning *et al.*, 1991) involve the presence or absence of the above-mentioned β-loop. Both the *Rb. sphaeroides* and *Rb. capsulatus* cytochromes contain the β-loop between amino acids 20 and 30 (*Rb. sphaeroides* numbering). In the cytochrome c_2 from *R. rubrum*, this β-loop is absent.

The hexagonal structure was used as the molecular replacement model to solve the triclinic and tetragonal crystal structures. The structures obtained were similar to that of the hexagonal structure with a root-mean-square overlap of 0.6 Å between corresponding C^{α} positions (not shown). The major difference observed was in the ligands of the heme prosthetic group (Fig. 3). In the triclinic and tetragonal crystal forms, the iron atom is coordinated at the axial ligand positions to the S atom of Met100 and the imidazole N atom of His19 (Fig. 3*a*). Such coordination of an invariant histidine residue and an invariant methionine residue to the heme iron is found in all class I *c*-type cytochromes (reviewed in Moore & Pettigrew, 1990, ch. 4). In the hexagonal crystal form, a discontinuity of the electron density between the heme Fe atom and the Met100 side chain was observed in the initial SIRAS maps and throughout the refinement process. This indicates a larger distance between the S atom of Met100 and the heme iron in the hexagonal form, *i.e.* 5.7 *versus* 2.3 Å found in the triclinic and tetragonal structures.

When the maps of the hexagonal crystal form were closely inspected, the existence of electron density that fits the geometry of a five-membered ring was observed (Fig. 3*b*). An imidazole molecule (from the crystallization buffer) (labeled in green in Fig. 3*b*) was positioned into this density, and a distance of 2.0 Å between the imidazole N atom and the Fe atom of the heme was determined. In addition, a bound water molecule (not shown), unique to the hexagonal form, was detected in the vicinity of the imidazole molecule. This water molecule can form hydrogen-bond interactions with the protein backbone and the imidazole that may further stabilize the binding of imidazole.

The structural evidence provided here for the binding of imidazole to the heme Fe atom and the displacement of the Met axial ligand of the cytochrome c_2 of *Rb. sphaeroides*, confirms previous findings in other systems. Schejter & George (1964) were the first to report the reaction between horse ferricytochrome *c* and imidazole. This interaction was characterized in a kinetic study by Sutin & Yandell (1972). The crystallographic structure is also in good agreement with the findings in the photosynthetic bacterium *Rb. capsulatus* where kinetic measurements indicated the binding of imidazole to cytochrome c_2 in solution (Hazzard, Caffrey, Myer & Cusanovich, 1992).

From the optical absorption spectrum of solubilized $P6_122$ hexagonal crystals, we determined that the cytochrome was in its oxidized (Fe^{3+}) form. This is in agreement with the findings of Schejter & Aviram (1969) who found a preferential binding of imidazole to the cytochrome in the Fe^{3+} oxidation state of the heme iron.

When the hexagonal crystals of cytochrome c_2 were soaked in low concentrations of sodium ascorbate (a reducing agent), the crystals remain physically intact but lose the capacity to diffract X-rays. Furthermore, growth of hexagonal crystals in the presence of imidazole from reduced (Fe^{2+}) protein occurred very slowly, over a period of 2–3 weeks, during which time the oxidation of the Fe^{2+} probably occurred. In contrast, growth of hexagonal crystals from oxidized (Fe^{3+}) protein, prepared under the same conditions, occurred overnight.

These findings indicate that redox-dependent ligand binding can alter the crystallization properties and the quality of diffraction of the resulting crystals. Ligand substitution of buffers like imidazole may be of importance in the crystallization as well as the function of other metalloproteins.*

We thank Tim Donohue for providing the cytochrome c_2 overproducing strain, Hazel Holden for providing trimethyllead acetate used in the heavy-atom soaks and N.-H. Xuong for providing access to X-ray precession camera facilities at UCSD. We thank Rachel Nechustai for critical comments on the manuscript; Hiromi Komiya for providing helpful advice on the crystallographic model building; Ed Abresch and Roger Isaacson for technical assistance; and Noam Adir, Robert Bartsch, Mel Okamura and Scott Rongey for helpful discussions. This work has been supported by the National Institutes of Health (GM13191, GM45162 and GM41300) and the United States Department of Agriculture Cooperative State Research Service (93-37306-9182). HLA has been partially supported by a National Institute of Health Postdoctoral Training Grant (5T32 DK07233-16).

Note added in proof: The cytochrome c_2 structure presented in this work was used to determine the preliminary structure of a reaction center–cytochrome c_2 complex from *Rb. sphaeroides* (Adir, Okamura & Feher, 1994).

* Atomic coordinates and structure factors of the hexagonal crystal (Reference: 1CXA, R1CXASF), the triclinic crystal (Reference: 1CXB, R1CXBSF) and the tetragonal crystal (Reference: 1CXC, R1CXCSF) have been deposited with the Protein Data Bank, Brookhaven National Laboratory. Free copies may be obtained through The Technical Editor, International Union of Crystallography, 5 Abbey Square, Chester CH1 2HU, England (Supplementary Publication No. SUP 37116).

References

ADIR, N., OKAMURA, M. Y. & FEHER, G. (1994). *Biophys. J.* **66**, A228 (Abstract).

ALLEN, J. P. (1988). *J. Mol. Biol.* **204**, 495–496.

ALLEN, J. P., FEHER, G., YEATES, T. O., KOMIYA, H. & REES, D. C. (1987). *Proc. Natl Acad. Sci. USA*, **84**, 6162–6166.

ALLEN, J. P., FEHER, G., YEATES, T. O., REES, D. C., DEISENHOFER, J., MICHEL, H. & HUBER, R. (1986). *Proc. Natl Acad. Sci. USA*, **83**, 8589–8593.

AMBLER, R. P., DANIEL, M., HERMOSO, J., MEYER, T. E., BARTSCH, R. G. & KAMEN, M. D. (1979). *Nature (London)*, **278**, 659–660.

AXELROD, H., FEHER, G., ALLEN, J. P., DAY, M., CHIRINO, A., HSU, B. T. & REES, D. C. (1992*a*). *Biophys. J.* **61**, 595 (Abstract).

AXELROD, H., FEHER, G., ALLEN, J. P., DAY, M., CHIRINO, A., HSU, B. T. & REES, D. C. (1992*b*). Am. Crystallogr. Assoc. Annu. Meet., Pittsburgh, Abstract PC35.

BARTSCH, R. G. (1978). *The Photosynthetic Bacteria*, edited by R. K. CLAYTON & W. R. SISTROM, ch. 13, pp. 249–279. New York: Plenum Press.

BENNING, M. M., WESENBERG, G., CAFFREY, M. S., BARTSCH, R. G., MEYER, T. E., CUSANOVICH, M. A., RAYMENT, I. & HOLDEN, H. M. (1991). *J. Mol. Biol.* **220**, 673–685.

BRANDNER, J. P., MCEWAN, A. G., KAPLAN, S. & DONOHUE, T. J. (1989). *J. Bacteriol.* **171**, 360–368.

BRÜNGER, A. T., KURIYAN, J. & KARPLUS, M. (1987). *Science*, **235**, 458–460.

CAFFREY, M. S., BARTSCH, R. G. & CUSANOVICH, M. A. (1992). *J. Biol. Chem.* **267**, 6317–6321.

CHANG, C.-H., EL-KABBANI, O., TIEDE, D., NORRIS, J. & SCHIFFER, M. (1991). *Biochemistry*, **30**, 5352–5360.

CHANG, C.-H., TIEDE, D., TANG, J., SMITH, U., NORRIS, J. & SCHIFFER, M. (1986). *FEBS Lett.* **205**, 82–86.

CROFTS, A. R. & WRAIGHT, C. A. (1983). *Biochim. Biophys. Acta*, **726**, 149–185.

DEISENHOFER, J., EPP, O., MIKI, K., HUBER, R. & MICHEL, H. (1985). *Nature (London)*, **318**, 618–624.

FEHER, G. & OKAMURA, M. (1978). *The Photosynthetic Bacteria*, edited by R. K. CLAYTON & W. R. SISTROM, ch. 19, pp. 349–386. New York: Plenum Press.

FITZGERALD, P. M. D. (1988). *J. Appl. Cryst.* **21**, 273–278.

HAZZARD, J. H., CAFFREY, M. S., MYER, A. B. & CUSANOVICH, M. A. (1992). *Biophys. J.* **61**, 201 (Abstract).

HIGASHI, T. (1990). *PROCESS: a Program for Indexing and Processing R-AXIS* II *Imaging Plate Data*. Rigaku Corporation, Tokyo, Japan.

HOLDEN, H. M. & RAYMENT, I. (1991). *Arch. Biochem. Biophys.* **291**, 187 194.

HOWARD, A. J., GILLILAND, G. L., FINZEL, B. C., POULOS, T. L., OHLENDORF, D. H. & SALEMME, F. R. (1987). *J. Appl. Cryst.* **20**, 383–387.

JONES, T. A. (1985). *Methods Enzymol.* **115**, 157 171.

KRAULIS, P. J. (1991). *J. Appl. Cryst.* **24**, 946–950.

MCPHERSON, A. (1982). *Preparation and Analysis of Protein Crystals*. New York: Wiley.

MATTHEWS, B. W. (1968). *J. Mol. Biol.* **33**, 491–497.

MEYER, T. E. (1970). PhD thesis. Univ. of California, San Diego, USA.

MOORE, G. R. & PETTIGREW, G. W. (1990). *Cytochromes c, Evolutionary, Structural, Physiochemical Aspects*. Berlin: Springer-Verlag.

NICHOLLS, D. G. & FERGUSON, S. J. (1992). *Bioenergetics* 2. London: Academic Press.

OVERFIELD, R. E., WRAIGHT, C. A. & DEVAULT, D. (1979). *FEBS Lett.* **105**, 137–142.

PRINCE, R. C., BACCARINI-MELANDRI, A., HAUSKA, G. A., MELANDRI, B. A. & CROFTS, A. R. (1975). *Biochim. Biophys. Acta*, **387**, 212–227.

PRINCE, R. C., COGDELL, R. J. & CROFTS, A. R. (1974). *Biochim. Biophys. Acta*, **347**, 1–13.

REEKE, G. N. (1984). *J. Appl. Cryst.* **17**, 125–130.

ROSEN, D., OKAMURA, M. Y., ABRESCH, E. C., VALKRIS, G. E. & FEHER, G. (1983). *Biochemistry*, **22**, 335–341.

ROSEN, D., OKAMURA, M. Y. & FEHER, G. (1980). *Biochemistry*, **19**, 5687–5692.

ROTT, M. A., FITCH, J., MEYER, T. E. & DONOHUE, T. J. (1992). *Arch. Biochem. Biophys.* **292**, 576–582.

SALEMME, F. R., FREER, S. T., XUONG, N.-H., ALDEN, R. A. & KRAUT, J. (1973). *J. Biol. Chem.* **248**, 3910–3921.

SCHEJTER, A. & AVIRAM, I. (1969). *Biochemistry*, **8**, 149–153.

SCHEJTER, A. & GEORGE, P. (1964). *Biochemistry*, **3**, 1045–1049.

SUTIN, N. & YANDELL, J. K. (1972). *J. Biol. Chem.* **247**, 6932–6936.

TERWILLIGER, T. C. & EISENBERG, D. (1983). *Acta Cryst.* A**39**, 813–817.

THORNBER, J. P., OLSON, J. M., WILLIAMS, D. M. & CLAYTON, M. L. (1969). *Biochim. Biophys. Acta*, **172**, 351–354.

TIEDE, D. M. & CHANG, C.-H. (1988). *Isr. J. Chem.* **28**, 183–191.

TRONRUD, D. E., TENEYCK, L. F. & MATTHEWS, B. W. (1987). *Acta Cryst.* A**43**, 489–501.

VENKATACHALAN, C. M. (1968). *Biopolymers*, **6**, 1425–1436.

VERNON, L. P. & KAMEN, M. D. (1954). *J. Biol. Chem.* **211**, 643–662.